FEBS Letters 575 (2004) 86–90 FEBS 28788

Is the cytoplasmic loop of MerT, the mercuric ion transport protein, involved in mercury transfer to the mercuric reductase?

Emmanuel Rossy[a,e], Olivier Sénèque[b], David Lascoux[c], David Lemaire[c], Serge Crouzy[d], Pascale Delangle[b], Jacques Covès[e,*]

[a]*Laboratoire de Chimie et Biochimie des Centres Redox Biologiques, DRDC/CB, CEA-Grenoble, France*
[b]*Laboratoire de Reconnaissance Ionique, DRFMC/SCIB, CEA-Grenoble, France*
[c]*Laboratoire de Spectrométrie de Masse des Protéines, Institut de Biologie Structurale, Grenoble, France*
[d]*Laboratoire de Biophysique Moléculaire et Cellulaire, DRDC/BMC CEA-Grenoble, France*
[e]*Laboratoire des Protéines Membranaires, Institut de Biologie Structurale (IBS), UMR 5075 CNRS, CEA, Université Joseph Fourier, 41 Rue Jules Horowitz, 38027 Grenoble Cedex, France*

Received 24 June 2004; revised 12 August 2004; accepted 16 August 2004

Available online 2 September 2004

Edited by Maurice Montal

Abstract In MerT, the mercury transporter, a first cysteine pair, located in the first *trans*-membrane helix, receives mercury from the periplasm. Then, a second cysteine pair, housed in a cytoplasmic loop connecting the second and the third *trans*-membrane helices, is thought to transfer the metal to another cysteine pair located in the N-terminal extension of the mercuric reductase. We found that a 23-amino acid synthetic peptide corresponding to the cytoplasmic loop can bind one mercury atom per molecule and that this mercury atom can be transferred specifically to MerAa. The solution structure of Hg-bound ppMerT has been solved by ^{1}H NMR spectroscopy.

Keywords: Mercury transport; Heavy-metal resistance; Mass spectrometry; ^{1}H NMR spectroscopy; *Ralstonia metallidurans* CH34

1. Introduction

The facultative autotrophic bacterium *Ralstonia metallidurans* CH34 contains at least two copies of the canonic *merRTPAD* operons conferring narrow-spectrum resistance to inorganic mercury [1]. The *merTPA* genes encode the proteins responsible for the periplasmic sequestration of Hg(II) (MerP), the transport through the inner membrane of the metal into the cytoplasm (MerT) and the reduction of inorganic mercury to the less toxic elemental mercury (MerA, the cytosolic mercuric reductase) [2]. The products of the genes *merR* and *merD* play crucial roles at the regulatory level [3,4]. MerP, MerT and MerA are supposed to interact, at least transiently, in order to drive mercury to the catalytic core of the reductase [5–7]. The role of these proteins has been assessed by diverse genetic techniques, including both random and site-directed mutagenesis, and analysis of the corresponding phenotypes [8–13]. MerT alone has been demonstrated to be required for mercury transport even if the uptake of Hg(II) is more efficient along with MerP [12]. Certain paired cysteines have been identified to be essential for mercury transfer, while the role of other cysteine pairs remains unclear. MerT from *R. metallidurans* CH34 is homologous to that encoded by Tn*501* from *Pseudomonas aeruginosa*. They are predicted to contain three *trans*-membrane helices (TM). The first TM contains two adjacent cysteines essential for the transport [12,14]. Another cysteine pair is located in the peptide lying in the cytoplasm and connecting the second and third TM. The mutation of these cysteines in Tn*501*-encoded MerT causes a reduction of mercury transport [12,13]. In the same way, mutants of MerA, in which the two N-terminal cysteines were converted to alanines or serines, are still capable of mercuric reductase activity in vitro or mercury resistance in vivo [10,11,15]. The N-terminal extension of the mercuric reductase, called MerAa, has been structurally defined under the reduced and the Hg-bound forms, very recently [16]. The role of the cysteines in mercury binding was unambiguously demonstrated. MerAa is a MerP analog and its role could be to accept mercury from MerT and to transfer the metal to the catalytic core of the reductase [2,16].

We have used a 23-amino acid synthetic peptide corresponding to the cytoplasmic loop of MerT, and MerAa to study the transfer of mercury between the transport protein and the mercuric reductase. Our results argue in favor of a specific role of these peptides in metal exchange between the two proteins.

2. Materials and methods

2.1. Proteins, peptide and chemicals

MerAa and MerP were overexpressed, purified and reduced as previously described [16,17]. The 23-mer peptide (RRIYRQAAAC-KPGEVCAIPQVRA) called ppMerT in the following and corresponding to the cytoplasmic loop of MerT contains two cysteines. It was synthesized by NeoSystems (Strasbourg, France) under the linear form (reduced). GSH, L-cysteine and other chemicals were of the purest grade commercially available.

2.2. Mass spectrometry analysis of ppMerT and of its mercury binding and exchange capacities

Electrospray mass spectrometry (ESI-MS) was performed using Q-TOF Micromass spectrometer (Micromass, Manchester, UK) equipped with an electrospray ion source as previously described [16,17]. A stock solution of 1 mM ppMerT was prepared extemporaneously by

* Corresponding author. Fax: +33-4-38-78-54-94.
E-mail address: jacques.coves@ibs.fr (J. Covès).

0014-5793/$22.00 © 2004 Published by Elsevier B.V. on behalf of the Federation of European Biochemical Societies.
doi:10.1016/j.febslet.2004.08.041

dissolving the dry powder in sterile water. The stock solution was diluted to 100 μM in 50 mM Tris–HCl, pH 7.5. The peptide was then titrated by addition of increasing amounts of $HgCl_2$. The concentration of the mercury solution was calculated so that the added volume for each titration was negligible. ESI-MS spectra were recorded one minute after each addition of mercury.

For mercury transfer experiments, Hg-bound ppMerT was prepared by a single addition of 0.8 molar equivalent of metal and then diluted to 100 μM in 50 mM Tris–HCl, pH 7.5, containing 100 μM of one of the following protein: reduced MerAa, reduced MerP or myoglobin. Alternatively, the proteins were replaced with 8 mM of GSH or 200 μM of L-cysteine. After an incubation of 10 min at room temperature, the reaction was stopped by freezing the solution in liquid nitrogen before ESI-MS analysis.

2.3. NMR spectroscopy and structure calculation

^1H NMR spectra were recorded on a Bruker Avance spectrometer operating at 500 MHz at 298 K. Samples (1.1 mM) of the peptide (*apo*- or Hg-bound form) were prepared in D_2O/H_2O (1/9 v/v). Water suppression was achieved with the watergate pulse sequence [18,19]. TOCSY [20] spectra were collected with 70 ms mixing time, t-ROESY [21,22] with 100 ms mixing time (3300 Hz spin-lock), and NOESY experiments with 100, 200, 300 and 400 ms mixing times. Coupling constants ($^3J_{NH,H\alpha}$) were measured by Soft-COSY [23] experiments. ^{199}Hg NMR spectra were recorded on a Varian Mercury spectrometer operating at 71.6 MHz. For that purpose, a 2.4 mM solution of Hg-bound ppMerT was prepared using 91% enriched $^{199}Hg^{2+}$. Chemical shift of ^{199}Hg is reported relative to $Hg(CH_3)_2$ (0 ppm) [24].

Solution structures were calculated using the program X-PLOR 3.1 following standard refinement protocols [25]. Upper and lower limits for distance constraints were set to ±15% of the H–H distances obtained by integration of NOESY spectra (200 and 300 ms). Gly Hα1/Hα2 (1.78 Å), Pro Hδ1/Hδ2 (1.78 Å), Pro Hα/Hβ1 (2.36 Å) and Pro Hα/Hβ2 (2.70 Å) were used as references for distance calibration. Φ dihedral constraints were derived from $^3J_{HN,H\alpha}$ coupling constants. Pseudo-atom corrections were applied to non-stereospecifically assigned methylenes and methyl groups [26]. The S–Hg bond lengths were set to 2.33 Å, which is typical of linear bicoordinate RS–Hg–SR complexes [27,28]. No NOE violations greater than 0.3 Å and no dihedral angles violations greater than 5° were found.

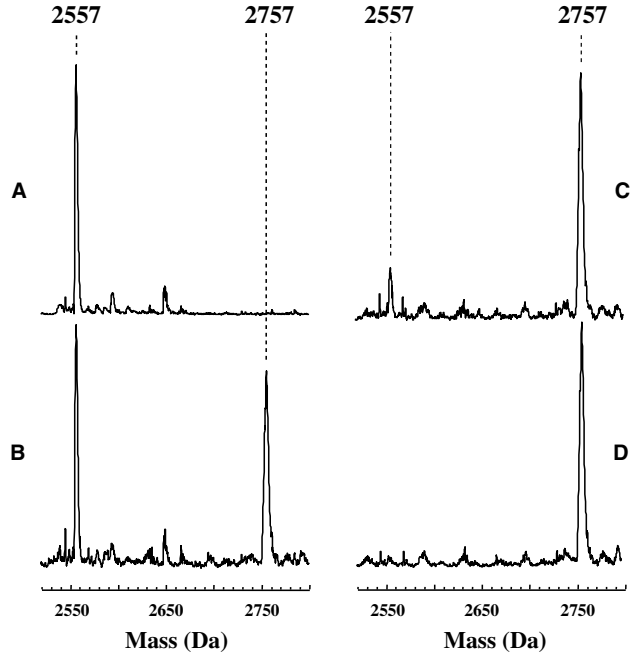

Fig. 1. ESI-MS titration of ppMerT with $HgCl_2$. (A) Synthetic linear ppMerT, (B–D) ppMerT + 0.5, 0.75 and 1 molar equivalent of $HgCl_2$. The mass of *apo*-ppMerT or Hg-bound ppMerT is reported at the head of each panel.

3. Results

3.1. Mercury binding capacity of ppMerT

Fig. 1 shows the reconstructed mass spectrum of ppMerT. The mass of 2557 Da fits perfectly the expected mass deduced from the amino acid sequence of ppMerT. As ppMerT was already reduced, it has been used directly for the binding experiments. Upon the first addition of 0.5 mercury equivalent, one extra peak appeared with a mass difference of 200 Da with respect to the ppMerT native mass. This corresponds to the addition of one mercury atom. As further mercury was added, the proportion of peptide with bound-mercury increased, while the proportion of the *apo*-form decreased. Finally, a full conversion to Hg-bound ppMerT is observed for one mercury equivalent. As previously observed for MerP or MerAa, the binding of the mercury is strong enough to resist the ESI-MS conditions [16,17].

3.2. Folding of ppMerT upon mercury binding

The solution structures of the *apo*- and Hg-bound forms of ppMerT were investigated by 1D and 2D ^1H NMR experiments (not shown). All NH resonances but one in the ^1H spectrum of *apo*-ppMerT (1.1 mM in H_2O/D_2O 9:1, pH 4.0) were in the [7.95 ppm, 8.45 ppm] window. The t-ROESY spectrum showed very few inter-residue correlations and the α protons of Gly13 were not differentiated. These data account for a fully unfolded *apo*-peptide. Upon addition of 1.1 eq. of $HgCl_2$, significant changes appeared in the ^1H NMR spectrum (Table 1). The decrease of the pH to 2.5 and the downfield shift of both cysteines (Cys10 and Cys16) Hβ protons (about 0.5 ppm) suggest a deprotonation of the sulfur groups and an involvement of the cysteines in mercury binding. A linear coordination of Hg^{2+} by the two cysteines was confirmed by the ^{199}Hg NMR chemical shift (−1008 ppm) of ppMerT-Hg [24]. We checked that the neighboring carboxylate of Glu14 was not coordinated to Hg^{2+} by raising the pH to 5.6 with NaOH. No change occurred in the spectrum except the up-field shift of

Table 1
^1H NMR (500 MHz) chemical shifts (δ ppm) for Hg-bound ppMerT (residues 10–17) in H_2O/D_2O at 298 K

Residue	HN	Hα	Hβ	Others
Cys10	8.27	4.41	3.30, 3.08	
Lys11	8.03	4.52	1.73, 1.49	$CH_2(\gamma)$: 1.36; $CH_2(\delta)$: 1.58; $CH_2(\varepsilon)$: 2.89
Pro12	–	4.25	2.21, 1.78	$CH_2(\gamma)$: 2.03, 1.90; $CH_2(\delta)$: 3.78,3.51
Gly13	8.67	4.09, 3.61		
Glu14	7.64	4.41	2.18, 1.96	$CH_2(\gamma)$: 2.38
Val15	8.50	4.03	2.01	$CH_2(\gamma)$: 0.86
Cys16	8.32	4.55	3.34, 3.29	
Ala17	8.32	4.29	1.28	

Glu14 Hγ due to the deprotonation of the COOH moiety. Concomitantly to mercury binding, the NH resonances of residues 10–16 were strongly shifted while the others were not, and a higher number of inter-residue NOEs were observed in this part of the peptide, thereby suggesting the structural organization of the CKPGEVC motif. Actually, characteristic elements of a type II β-turn structure for the KPGE sequence were identified: a *trans* peptide bond for proline (*d*(Lys11 Hα, Pro10 Hδ) = 2.2 Å), a *cis* relationship between Gly13 HN and Pro12 Hα (2.0 Å), and a relatively strong NOE cross-peak between Glu14 HN and Pro10 Hα (3.3 Å) [29]. However, all values of $^{3}J_{HN,H\alpha}$ couplings in the CKPGEVC motif were in the 6–8 Hz range except for Glu14 (8.5 Hz). Thus, although the CKPGEVC motif folds upon mercury binding, it remains flexible. As the two extensions beyond the cysteines were not structured upon mercury binding, only residues 9–17 were introduced in the structure calculations. Forty NOE-derived H–H distance constraints and one Φ dihedral constraint were used for the calculations. Fifty structures were calculated using X-PLOR 3.1 [25]. They had very similar energies and responded to the imposed constraints. A superimposition of the 20 lowest energy structures is shown in Fig. 2A. The β-turn (residues 11–14) is relatively rigid and consequently was rather well defined with an excellent superimposition of the 20 structures in this region (backbone RMSD: 0.67 Å). The other amino acids are more mobile as expected from the NMR analysis. The lowest energy structure depicted in Fig. 2B shows how ppMerT forms a cycle through mercury binding by the two cysteine sulfur atoms.

The complexation properties of ppMerT towards other metals (Zn^{2+}, Cd^{2+} and Pb^{2+}) have been investigated. As for Hg^{2+}, ESI-MS shows the formation of 1:1 complexes and ^{1}H NMR competition experiments showed that mercury quantitatively displaces the other three cations (not shown), thereby reflecting the specificity of ppMerT for Hg^{2+}.

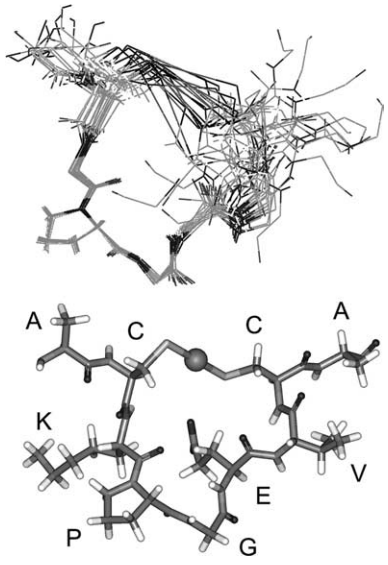

Fig. 2. Solution structure of Hg-bound ppMerT. Top panel: superimposition of the 20 lowest energy structures. Bottom panel: lowest energy structure of the ^{9}ACKPGEVCA^{17} sequence. The sphere represents the mercury atom and the amino acids are identified.

3.3. Exchange of mercury between ppMerT and putative partners

The initial ESI-MS spectrum of Hg-bound ppMerT used in metal exchange experiments is shown in Fig. 3A. Hg-bound ppMerT incubated with *apo*-MerAa was transformed essentially to the *apo*-form (Fig. 3B), while Hg-bound MerAa appeared along with *apo*-MerAa (Fig. 3E). The mass spectrum of MerAa (Fig. 3E) showed four peaks because this peptide was purified under two forms: with or without the initial methionine [16]. These two sub-populations have a mass difference of 131 Da and the *apo*- or the Hg-bound forms have a mass difference of 200 Da. In order to check the specificity of the metal transfer, several controls were performed. First, Hg-bound ppMerT was mixed with *apo*-MerP. MerP is a structural analog of MerAa and contains a similar mercury-binding domain [16,17]. However, under these conditions, only half of the ppMerT population lost its metal (Fig. 3C), while MerP remained essentially under the *apo*-form (Fig. 3F). Second, in the presence of 8 mM GSH, a concentration representing the physiological concentration of reduced glutathione in bacterial cytoplasm, a similar result was obtained, only half of ppMerT lost its metal (Fig. 3D). The same result was also obtained by incubating Hg-bound ppMerT with 200 μM of L-cysteine (not shown). Third, Hg-bound ppMerT was mixed with myoglobin, a protein without any relation with mercury binding. As a consequence, ppMerT remained essentially under the

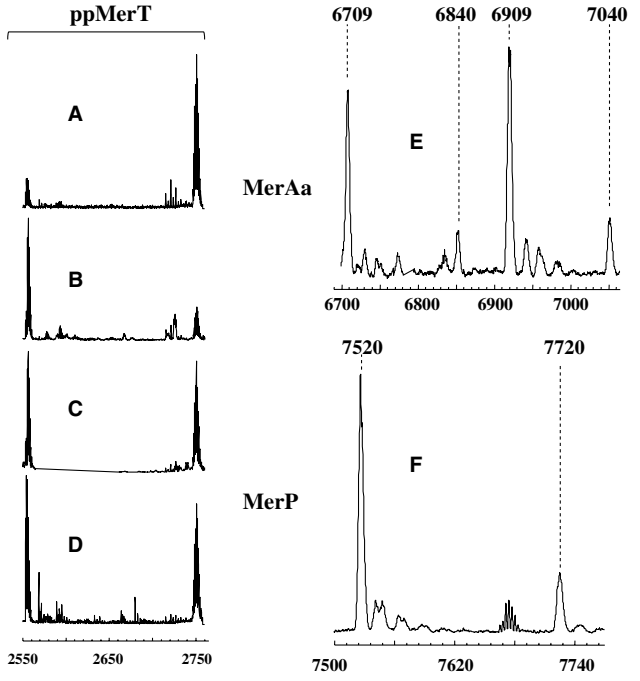

Fig. 3. Exchange of mercury between ppMerT and partners followed by ESI-MS. The conditions of incubation and analysis of the different components of the system are described in Section 2. The *ppMerT* panel shows (A) Hg-bound ppMerT obtained after incubation of 100 μM ppMerT with 80 μM $HgCl_2$, (B) Hg-bound ppMerT after incubation with 100 μM of MerAa, (C) 100 μM of MerP and (D) 8 mM of GSH. The masses of *apo*- and Hg-bound ppMerT are indicated in Fig. 1. The ESI-MS analyses of MerAa and MerP after incubation with Hg-bound ppMerT are depicted in panels E and F, respectively. The exact mass expressed in Da of the different forms of the proteins is indicated at the head of each panel.

Hg-bound form after the incubation with myoglobin (not shown).

4. Discussion

The present study focuses on the putative exchange of mercury between a 23-mer linear synthetic peptide mimicking the cytoplasmic loop of MerT and the N-terminal domain of MerA. Synthetic peptides mimicking the well-known metal-binding motif MxCxxC have already been used to delineate the structure or the metal selectivity of proteins such as MerP [27,30] or Atx1 [31]. In both cases, NMR was the method of choice. Interestingly, Opella and coworkers [32] found that a xxCC motif was much more specific for Hg(II) than the CxxC one. The xxCC motif found in the first TM of MerT could make the transport protein the central piece in selection of the metal to be incorporated by the bacterium [32]. We found that ppMerT is also specific for Hg(II) over the biologically relevant ion Zn^{2+}, or other toxic cations such as Cd^{2+} or Pb^{2+}. The binding of mercury is accompanied by the folding of ppMerT. The coordination-induced structural organization is favored by the presence of a proline–glycine motif in the CKPGEVC sequence that induces a β-turn bringing closer the two reactive cysteines. The two extensions beyond the cysteines were found to be highly flexible even in the presence of mercury. Such a flexibility is very unlikely in native MerT, since these extensions are directly connected to the second and third TM. One can thus describe the cytoplasmic loop as a pre-organized cyclic peptide rigidified by the β-turn and the fixation to the TM. Moreover, as the cytoplasm is known to provide a reductive environment, the thiol groups would be immediately ready for the coordination of the mercury atom.

We have also shown that mercury was easily exchangeable between Hg-bound ppMerT and *apo*-MerAa. The mass spectrometry analysis of ppMerT after mixture with *apo*-MerAa suggested an almost quantitative exchange of metal between the two peptides. It is noteworthy that, under these conditions, the solutions did not contain additional thiols such as the biologically relevant glutathione. This shows that GSH is dispensable for the transfer of mercury from MerT to MerAa, although a donor thiol ligand such as a Hg(II)-diglutathione adduct is required to provide Hg(II) to the catalytic core of the mercuric reductase for good reduction in vitro [2,10]. Actually, MerAa has the perfect size and shape [2,7,16] to play the role of such a protein dithiol Hg(II) chelator and could be directly involved in the transfer of Hg(II) to the cysteines of the active center. Interestingly, we have shown that 8 mM GSH did not cause the full demetallation of Hg-bound ppMerT. This suggests that MerAa is exquisitely designed to take mercury from the transporter. Even if the N-terminal extension of MerA can be absent in certain mercuric reductases [33], for the large majority of these enzymes, it is found in one or several copies. It has been hypothesized recently that MerAa may become critical under conditions of depletion of the cellular thiol pool and a correlation between the number of MerAa repeats and the ability of the cell to synthesize high concentrations of glutathione has been noted [2]. Cells with low cellular thiol concentration have double repeats, while cells synthesizing GSH at high concentration have only a single repeat. Our results are in full agreement with these hypotheses.

As the transfer of mercury between ppMerT and MerAa is fast and almost quantitative, we can conclude that the dissociation constant of Hg(II) for ppMerT is higher than the K_d of mercury for MerAa, which has been determined in the micromolar range [34]. However, it is noteworthy that MerP was not able to fully transform Hg-bound ppMerT to *apo*-ppMerT, although it shares with MerAa similar metal-binding domain, tri-dimensional structure and dissociation constant for mercury [35,36]. This could reflect a basic thermodynamic control of the metal exchange due to slight differences in dissociation constants. However, in vivo, the metal exchange between MerT and MerAa may be favored by a transient electrostatic interaction between the two partners. Indeed, the cytoplasmic loop of MerT bears several positively charged residues (1 lysine and 4 arginines) and the metal-binding domain of MerAa contains an acidic residue (GMTCDSC). These charged residues could participate in such an interaction leading to a more productive metal exchange.

In conclusion, our data are consistent with a direct role of the cytoplasmic loop of MerT and the N-terminal extension of MerA in mercury exchange between the two proteins. Moreover, it is very likely that the paired cysteines found in the C-terminal ends of MerF (two adjacent cysteines) or MerC (Cx_4C), two other mercury transport proteins [14], should have a similar role. Interestingly, the C-terminal ends of these two proteins are also considerably rich in lysines and arginines.

References

[1] Mergeay, M., Monchy, S., Vallaeys, T., Auquier, V., Benotmane, A., Bertin, P., Taghavi, S., Dunn, J., van der Lelie, D. and Wattiez, R. (2003) FEMS Microbiol. Rev. 27, 358–410.
[2] Barkay, T., Miller, S.M. and Summers, A.O. (2003) FEMS Microbiol. Rev. 27, 355–384.
[3] Brown, N.L., Stoyanov, J.V., Kidd, S.P. and Hobman, J.L. (2003) FEMS Microbiol. Rev. 27, 145–163.
[4] Champier, L., Duarte, V., Michaud-Soret, I. and Covès, J. (2004) Mol. Microbiol. 52, 1475–1485.
[5] Brown, N.L. (1985) Trends Biochem. Sci. 10, 400–403.
[6] Schiering, N., Kabsch, W., Moore, M.J., Distefano, M.D., Walsh, C.T. and Pai, E.F. (1991) Nature 352, 168–172.
[7] Miller, S.M. (1999) in: Flavins and Flavoproteins (Ghisla, S., Kroneck, P., Macheroux, P. and Sund, H., Eds.), pp. 863–870, Agency for Scientific Publication, Berlin.
[8] Nakahara, H., Silver, S., Miki, T. and Rownd, R.H. (1979) J. Bacteriol. 140, 106–114.
[9] Lund, P.A. and Brown, N.L. (1987) Gene 52, 207–214.
[10] Moore, M.J. and Walsh, C.T. (1989) Biochemistry 28, 1183–1194.
[11] Miller, S.M., Moore, M.J., Massey, V., Williams Jr., C.H., Distefano, M.D., Ballou, D.P. and Walsh, C.T. (1989) Biochemistry 28, 1194–1205.
[12] Morby, A.P., Hobman, J.L. and Brown, N.L. (1995) Mol. Microbiol. 17, 25–35.
[13] Hobman, J.L. and Brown, N.L. (1996) Mol. Gen. Genet. 250, 129–134.
[14] Wilson, J.R., Leang, C., Morby, A.P., Hobman, J.L. and Brown, N.L. (2000) FEBS Lett. 472, 78–82.
[15] Brown, N.L., Shih, Y.-C., Leang, C., Glendinning, K.J., Hobman, J.L. and Wilson, J.R. (2002) Biochem. Soc. Trans. 30, 715–718.
[16] Rossy, E., Champier, L., Bersch, B., Brutscher, B., Blackledge, M. and Covès, J. (2004) J. Biol. Inorg. Chem. 9, 49–58.
[17] Serre, L., Rossy, E., Pebay-Peyroula, E., Cohen-Addad, C. and Covès, J. (2004) J. Mol. Biol. 339, 161–171.
[18] Piotto, M., Saudek, V. and Sklenar, V. (1992) J. Biomol. NMR 2, 661–666.
[19] Sklenar, V., Piotto, M., Leppik, R. and Saudek, V. (1993) J. Magn. Reson. A 102, 241–245.
[20] Bax, A. and Davis, D.G. (1985) J. Magn. Reson. 65, 355–360.

[21] Desvaux, H., Berthault, P., Birlirakis, N., Goldman, M. and Piotto, M. (1995) J. Magn. Reson. A 113, 47–52.
[22] Malliavin, T.E., Desvaux, H. and Delsuc, M.-A. (1998) Magn. Reson. Chem. 36, 801–806.
[23] Brüschweiler, R., Madsen, J.C., Griesinger, C., Sørensen, O.W. and Ernst, R.R. (1987) J. Magn. Reson. 73, 380–385.
[24] Utschig, L.M., Bryson, J.W. and O'Halloran, T.V. (1995) Science 268, 380–385.
[25] Brünger, A.T. (1992) X-PLOR version 3.1. A System for X-ray Crystallography and NMR. Yale University Press, New Haven, CT.
[26] Fletcher, C.M., Jones, D.N.M., Diamond, R. and Neuhaus, D.J. (1996) Biomol. NMR 8, 292–310.
[27] Veglia, G., Porcelli, F., DeSilva, T.M., Prantner, A. and Opella, S.J. (2000) J. Am. Chem. Soc. 122, 2389–2390.
[28] Yamamura, T., Watanabe, T., Kikuchi, A., Yamane, T., Ushiyama, M. and Hirota, H. (1997) Inorg. Chem. 36, 4849–4859.
[29] Wüthrich, K., Billeter, M. and Braun, W. (1984) J. Mol. Biol. 180, 715–740.
[30] Opella, S.J., DeSilva, T.M. and Veglia, G. (2002) Curr. Opin. Chem. Biol. 6, 217–223.
[31] Sénèque, O., Crouzy, S., Boturyn, D., Dumy, P., Ferrand, M. and Delangle, P. (2004) Chem. Commun. 7, 770–771.
[32] DeSilva, T.M., Veglia, G., Porcelli, F., Prantner, A.M. and Opella, S.J. (2002) Biopolymers 64, 189–197.
[33] Sedlmeier, R. and Altenbuchner, J. (1992) Mol. Gen. Genet. 236, 76–85.
[34] Sahlman, L. and Jonsson, B.-H. (1992) Eur. J. Biochem. 205, 375–381.
[35] Steele, R.A. and Opella, S.J. (1997) Biochemistry 36, 6885–6895.
[36] Qian, H., Sahlman, L., Eriksson, P.-O., Hambraeus, C., Edlund, U. and Sethson, I. (1998) Biochemistry 37, 9316–9322.